Hindawi
Advances in Materials Science and Engineering
Volume 2020, Article ID 5649492, 13 pages
https://doi.org/10.1155/2020/5649492

Research Article

Sinking Velocity Impact-Analysis for the Carrier-Based Aircraft Using the Response Surface Method-Based Improved Kriging Algorithm

Xiao-Feng Xue,[1] **Yuan-Zhuo Wang**,[2] **Cheng Lu**,[1] **and Zhang Yun-Peng**[1]

[1]*School of Aeronautics, Northwestern Polytechnical University, Xi'an 710072, China*
[2]*School of Astronautics, Northwestern Polytechnical University, Xi'an 710072, China*

Correspondence should be addressed to Xiao-Feng Xue; xuexiaofeng@nwpu.edu.cn

Received 16 March 2020; Revised 30 March 2020; Accepted 20 April 2020; Published 7 May 2020

Guest Editor: Shun-Peng Zhu

The deck landing sinking velocity of carrier-based aircraft is affected by carrier attitude, sea condition, aircraft performance, etc. Its impact analysis is a complex nonlinear problem, and there even is some contradictory phenomenon that when the approach velocity increases, the sinking velocity decreases under certain circumstances. Aiming at exploring the impact of the various related deck landing parameters on sinking velocity for carrier-based aircraft in the actual environment, response surface method-based improved Kriging algorithm (IK-RSM) is proposed based on genetic algorithm and Kriging model. Based on the deck landing measured data of the F/A-18A aircraft in the actual operating environment, the impact degree of the 15 deck landing parameters on the sinking velocity is explored, respectively, by using the partial correlation analysis of multivariate statistical theory and the IK-RSM. It can be found that the 4 parameters are strongly correlated with the sinking velocity; that is, the aircraft glide angle and deck pitch angle are highly correlated with the sinking velocity; next, the approach velocity and the engaging velocity are moderately correlated with the sinking velocity. The 4 parameters above could be used to establish the impact analysis model of the sinking velocity. The genetic algorithm is applied to the correction coefficients optimization of the IK-RSM's kernel functions, and the IK-RSM of the F/A-18A aircraft sinking velocity is formed. Compared with the Kriging model and the empirical formula, the sinking velocity prediction accuracy indexes of IK-RSM are the best; for example, the determination coefficient is 0.981, the mean relative error is 1.813%, and the maximum relative error is 6.771%. Furthermore, based on the sinking velocity IK-RSM and the sensitivity analysis method proposed, we have explained the reason for the contradictory phenomenon that when the approach velocity increases, the sinking velocity decreases at some samples. It could provide certain technical support for the flight attitude control related to the sinking velocity during the actual flight of carrier-based aircraft.

1. Introduction

Sinking velocity is defined as the component of the aircraft velocity in vertical direction in the deck landing process of the carrier-based aircraft, which is an important design parameter for the landing gear [1]. The sinking velocity is the indication of the impact degree in the aircraft landing, and the range of which will seriously influence the weight of the landing gear and airframe structure. If the design value of sinking velocity is too small, this may lead to the aircraft structure being too weak and unable to reach the reliability requirement. Reversely, if the design value of sinking velocity is too large, this may lead to the aircraft structure being too heavy and further affects the aircraft flight performance. The deck landing sinking velocity of carrier-based aircraft is affected by many factors, such as aircraft carrier attitude, sea condition, and aircraft performance. So, the uncertainty will be too great to assess the value of sinking velocity under the influencing factors above. Therefore, it is urgent to carry out the impact-analysis research of the sinking velocity to reasonably design the relevant parameters of landing gear and guarantee the safety of carrier-based aircraft furthermore.

There have been quite a large body of literatures on carrier-based aircraft, and various theories and techniques have been developed. References [2, 3] studied the statistical features of the sinking velocity for carrier-based aircraft, which include the distribution characteristics and the empirical formula for calculating the mean and standard deviation. Micklos [4] investigated running state of carrier-based aircraft under considering different operational conditions and further provided the measured data. The statistical data show that there are many factors influencing the sinking velocity including 15 deck landing parameters, and the relationship between the sinking velocity and the corresponding influencing factors is highly nonlinear. In certain cases, there also is a contradictory phenomenon that the approach velocity increases and the sinking velocity decreases. Geng et al. [5] applied flight dynamics model of carrier aircraft to analyze the effect of the response time of engine, wave-off requirements, elevator efficiency, and deflection rate on the sinking velocity. Xia et al. [6] proposed an improved linearization method to correctly emulate aircraft groundspeed variations. Wang et al. [7] established the landing dynamics model and used finite element method to study the aircraft deck landing. Zhu et al. [8] built an actual model of arresting hook to investigate the influence on collision process under the deck friction. Wang et al. [9] employed realistic mechanisms and strategies to establish a model for carrier landing operations and studied the sinking velocity with pilot behavior. Zhang et al. [10] discussed the carrier-based aircraft landing laws that landed on the carrier by using the dynamics model of carrier-based aircraft landing gears that landed on moved deck. Wang et al. [11] and Yang et al. [12] evaluated the safety carrier-based aircraft ski-jump takeoff by the integrated dynamic simulation models of multibody system and nonlinear model. Yue et al. [13] studied the flow field of exhaust jets and its impact on the flight deck to provide some references for suitability of carrier-based aircrafts. Yin et al. [14] used simulated model to verify the deck movement and ship wake in the landing process of carrier-based aircraft. Wang et al. [15] developed an adaptive disturbance rejection algorithm to discuss the carrier-based aircraft dynamics and the linearized longitudinal model under turbulence conditions. Although the above efforts investigated the carrier-based aircraft from different perspectives, there are still some shortcomings on the sinking velocity study: (1) it has only provided the measured data of different kinds of carrier-based aircrafts considering different working conditions without including the relevant influence factors on the sinking velocity; (2) it has only finished the deterministic analysis of carrier-based aircraft by dynamic analysis theories without considering the randomness of influential factors, especially the sinking velocity; (3) most of works investigate the sinking velocity of carrier-based aircraft on the basis of theoretical methods without verifying the feasibility and applicability in engineering compounded with the measured data. Additionally, multiple disciplines need to be considered in the landing process of carrier-based aircraft, which include flight dynamics, aircraft control, and structural design. Hence, it is necessary to study the influence of the related parameters by numerical method, for instance, flight attitude, aircraft type, landing time (day/night), carrier motion, and sea conditions, on the sinking velocity. The sinking velocity of the carrier aircraft will be accurately determined. Due to the large number of parameters involved in the analysis and the high dimension, the traditional Kriging model is probable to fall into the local optimum in the process of solving the correction coefficient, which leads to some error between the prediction result and the measured value [16, 17]. Therefore, it is necessary to find a suitable method to establish a mathematical model between various factors and the sinking velocity to study the influence degree of each factor. Therefore, the goal of this paper is oriented to explore an analytical technique to study the sinking velocity of carrier-based aircraft, response surface method-based improved Kriging algorithm (IK-RSM), which integrates genetic algorithm and Kriging model, for the impact analysis and sensitivity analysis of carrier-based aircraft sinking velocity.

Based on the deck landing statistical data of the carrier-based aircraft F/A-18A, by using multivariate partial correlation analysis method, the key correlated parameters of the sinking velocity are identified, including the approach velocity, the engaging velocity, the glide angle, and the deck pitch angle. Then, the Kriging interpolation model and genetic algorithm are used to establish the IK-RSM model between the sinking velocity and the key correlated parameters mentioned above. The analysis of the sensitivity of each parameter to sinking velocity is carried out. An impact-analysis method for the carrier-based aircraft's sinking velocity based on measured data is developed and will provide technical support for the carrier-based aircraft design and research.

2. Partial Correlation Analysis Method for Determining the Key Correlated Parameters

Correlation analysis is firstly applied to study the correlation relationship among natural phenomena and explore the correlative direction and degree among the correlated stochastic phenomena [18, 19]. Subsequently, the relationship of multiple parameters is performed by correlation analysis. There are various technologies for correlation analysis, which mainly include chart analysis, covariance analysis, correlation coefficient analysis, regression analysis, and information entropy analysis. The correlation coefficient analysis is selected to finish the correlation analyses of the sinking velocity of carrier-based aircraft because this technique can judge and determine the correlation degrees between research object and influential factors. For multiple parameters involved in the process of influential parameter analyses for the sinking velocity of carrier-based aircraft, partial correlation analysis method is utilized. The basic principle of partial correlation analysis method is to individually investigate the correlation degree of two factors without considering the effects of other influential factors.

The correlation coefficient is the statistic index for the correlative degree between two variables, whose range is $[-1, 1]$. Hereinto, the correlation coefficients are positive or negative values. The positive value reveals that the outputs produce a positive variety with input variable, and vice versa. The correlation coefficient $r = 1$ illustrates that the two variables have completely linear correlation, $r = -1$ reveals that the two

variables have perfect negative correlation, and $r = 0$ expresses that the two variables do not have certainly linear dependence. $|r| \geq 0.8$ indicates that the variables are highly correlated, $0.5 \leq |r| < 0.8$ means the variables are moderately correlated, $0.3 \leq |r| < 0.5$ indicates that the variables are lowly correlated, and $|r| < 0.3$ denotes the variables are weakly correlated [20].

The measure indexes of partial correlation analysis are, respectively, first-order partial correlation coefficient, second-order partial correlation coefficient, and higher-order partial correlation coefficient, and the computational theories of these coefficients are listed as follows.

(1) First-order partial correlation coefficient reflects the correlative degree between two variables without considering the influence of another variable, which is expressed as

$$r_{ij-h} = \frac{r_{ij} - r_{ih}r_{jh}}{\sqrt{\left(1 - r_{ih}^2\right)\left(1 - r_{jh}^2\right)}}, \tag{1}$$

where r_{ij} is the correlation coefficient between x_i and x_j; r_{ih} is the correlation coefficient between x_i and x_h; r_{jh} is the correlation coefficient between x_j and x_h.

(2) Second-order partial correlation coefficient indicates the correlative degree between two variables without considering the effects of two other variables, x_h and x_m, which is expressed as

$$r_{ij-hq} = \frac{r_{ij-h} - r_{iq-h}r_{jq-h}}{\sqrt{\left(1 - r_{iq-h}^2\right)\left(1 - r_{jq-h}^2\right)}}, \tag{2}$$

where r_{ij-hq} is the second-order partial correlation coefficient indicating the correlative degree between two variables without considering the effects of two other variables, x_h and x_q.

(3) Higher-order partial correlation coefficient is applied to study the correlative degree between two variables considering the existence of multiple variables. Assuming that there are k variables, namely, $x_1, x_2, \ldots, x_k$, the $g\,(g \leq k-2)$-order partial correlation coefficient between x_i and x_j can be expressed as follows:

$$r_{ij-l_1l_2\cdots l_g} = \frac{r_{ij-l_1l_2\cdots l_{g-1}} - r_{il_g-l_1l_2\cdots l_{g-1}}r_{jl_g-l_1l_2\cdots l_{g-1}}}{\sqrt{\left(1 - r_{il_g-l_1l_2\cdots l_{g-1}}^2\right)\left(1 - r_{jl_g-l_1l_2\cdots l_{g-1}}^2\right)}}, \tag{3}$$

where $r_{ij-l_1l_2\cdots l_{g-1}}$, $r_{il_g-l_1l_2\cdots l_{g-1}}$, and $r_{jl_g-l_1l_2\cdots l_{g-1}}$ are the $g-1$ order partial correlation coefficients.

The correlation between two variables can be determined by the hypothesis test; that is,

$$\begin{cases} H_0\colon r = 0 \leftrightarrow H_1\colon r \neq 0, \\ t = \dfrac{r\sqrt{m-k-2}}{\sqrt{1-r^2}}, \\ p = P\{x \geq |t|\}, \end{cases} \tag{4}$$

and here m is the number of samples; $m-k-2$ is the degree of freedom; r is the g-order partial correlation coefficient. If the associated probability value p is less than the significant level, the null hypothesis is rejected that the correlation between the two variables is significant; otherwise, the null hypothesis is accepted due to no significant correlation between the two variables.

3. Parameter Impact Analysis Method Based on Improved Kriging Response Surface Model

With the help of the good interpolation characteristics of the IK-RSM, the influential factors of the sinking velocity and their laws will be discussed.

3.1. Mathematical Model of IK-RSM

3.1.1. Interpolation Form. IK-RSM is developed from RSM combined with the principles of genetic algorithm and Kriging model; the mathematical model of IK-RSM, namely, that response surface function-based improved Kriging algorithm (IK-RSF), includes linear regression function and nonparametric equation. For an unknown function $y(\mathbf{x})$, if the function value $y_i = y(\mathbf{x}_i)$ at the m design sites $\mathbf{x}_i (i = 1, 2, \ldots, m)$ is known in the domain Ω, then the Kriging model $\widehat{y}(\mathbf{x})$ of the unknown function could be expressed as follows:

$$\widehat{y}(\mathbf{x}) = F(\boldsymbol{\beta}, \mathbf{x}) + z(\mathbf{x}) = \mathbf{f}^T \cdot \boldsymbol{\beta} + z(\mathbf{x}), \tag{5}$$

where $F(\boldsymbol{\beta}, \mathbf{x})$ and $z(\mathbf{x})$ are quadratic polynomial regression model and random function, respectively. $F(\boldsymbol{\beta}, \mathbf{x})$ is denoted by vector expression; that is, $\mathbf{f}^T \cdot \boldsymbol{\beta}$ is the polynomial regression model; $\mathbf{f} = [\mathbf{f}_1(\mathbf{x}), \mathbf{f}_2(\mathbf{x}), \ldots, \mathbf{f}_p(\mathbf{x})]^T$ is the regression basis function for $\mathbf{x}$ and is expressed as the polynomial of $\mathbf{x}$. $\boldsymbol{\beta}$ is the coefficient vector of the regression basis function, and p is the number of regression basis functions, which is related to the number of independent variables and the form of the regression basis function selected. $z(\mathbf{x})$ is the error item formed by a stochastic process to correct the model. Therefore, the Kriging model $\widehat{y}(\mathbf{x})$ is the sum of the deterministic regression $\mathbf{f}^T \cdot \boldsymbol{\beta}$ and the approximation deviation $z(\mathbf{x})$.

3.1.2. Error Correction. The stochastic process $z(\mathbf{x})$ included in the mathematical model of IK-RSM (see equation (5)) (e.g., IK-RSF) is normal distribution; the mean and variance are 0 and σ^2, respectively. However, the value of covariance is not equal to 0; the mean, the variance, and covariance of $z(\mathbf{x})$ are written as follows:

$$\begin{aligned} E[z(\mathbf{x})] &= 0, \\ \mathrm{Var}[z(\mathbf{x})] &= \sigma^2, \\ \mathrm{cov}\left(z(\mathbf{x}_i), z\left(\mathbf{x}_j\right)\right) &= \sigma^2 R\left(\boldsymbol{\theta}, \mathbf{x}_i, \mathbf{x}_j\right), \end{aligned} \tag{6}$$

where $R(\boldsymbol{\theta}, \mathbf{x}_i, \mathbf{x}_j)$ is the correlation model for the arbitrary samples $\mathbf{x}_i$ and $\mathbf{x}_j$ with parameter $\boldsymbol{\theta}$; $\{\mathbf{x}_i\}_{i=1, 2, \ldots, m}$ and $\{\mathbf{x}_j\}_{j=1, 2, \ldots, m}$ are the vectors of the ith and jth random input variable; m is the number of training samples; σ^2 indicates

the process variance. The form of $R(\boldsymbol{\theta}, \mathbf{x}_i, \mathbf{x}_j)$ is denoted in equation (7).

$$R\left(\boldsymbol{\theta}, \mathbf{x}_i, \mathbf{x}_j\right) = \prod_{k=1}^{n} R\left(\boldsymbol{\theta}_k, \mathbf{x}_{i,k} - \mathbf{x}_{j,k}\right), \quad n \text{ is the number of variables,} \tag{7}$$

where $\mathbf{x}_{i,k}$ and $\mathbf{x}_{j,k}$ are the kth components of ith and jth random input variable, respectively; $R(\boldsymbol{\theta}_k, \mathbf{x}_{i,k} - \mathbf{x}_{j,k})$ is kernel function. Kernel function has many forms like Gaussian, exponential, linear, cubic, and so forth. Gaussian function is selected in this paper due to high computational accuracy in Kriging algorithm. Thus, equation (7) is restructured by

$$R\left(\boldsymbol{\theta}, \mathbf{x}_i, \mathbf{x}_j\right) = \exp\left[-\sum_{k=1}^{n} \boldsymbol{\theta}_k \left(\mathbf{x}_{i,k} - \mathbf{x}_{j,k}\right)^2\right], \tag{8}$$

where θ is the correction coefficient for the kernel function. Then, the kernel function matrices $\mathbf{R}$ could be gained by training samples. $\mathbf{R}$ is displayed by

$$\mathbf{R} = \begin{bmatrix} R\left(\boldsymbol{\theta}, \mathbf{x}_1, \mathbf{x}_1\right) & R\left(\boldsymbol{\theta}, \mathbf{x}_1, \mathbf{x}_2\right) & \cdots & R\left(\boldsymbol{\theta}, \mathbf{x}_1, \mathbf{x}_m\right) \\ R\left(\boldsymbol{\theta}, \mathbf{x}_2, \mathbf{x}_1\right) & R\left(\boldsymbol{\theta}, \mathbf{x}_2, \mathbf{x}_2\right) & \cdots & R\left(\boldsymbol{\theta}, \mathbf{x}_2, \mathbf{x}_m\right) \\ \vdots & \vdots & \ddots & \vdots \\ R\left(\boldsymbol{\theta}, \mathbf{x}_m, \mathbf{x}_1\right) & R\left(\boldsymbol{\theta}, \mathbf{x}_m, \mathbf{x}_2\right) & \cdots & R\left(\boldsymbol{\theta}, \mathbf{x}_m, \mathbf{x}_m\right) \end{bmatrix}_{m \times m}, \tag{9}$$

and here $R(\boldsymbol{\theta}, \mathbf{x}_i, \mathbf{x}_j)$ can be required from equation (8).

3.1.3. Polynomial Regression Basis Function. There are three forms for the regression polynomial models with the orders 0, 1, and 2 for the IK-RSM. The details are as follows.

Constant, $p = 1$:

$$f_1(x) = 1. \tag{10}$$

Linear, $p = n + 1$:

$$f_1(\mathbf{x}) = 1, \quad f_2(\mathbf{x}) = \mathbf{x}_1, \ldots, f_{n+1}(\mathbf{x}) = x_n. \tag{11}$$

Quadratic, $p = 1/2\,(n+1)\,(n+2)$:

$$\begin{aligned} &f_1(\mathbf{x}) = 1, \\ &f_1(\mathbf{x}) = 1, f_2(\mathbf{x}) = \mathbf{x}_1, \ldots, f_{n+1}(\mathbf{x}) = \mathbf{x}_n, \\ &f_{n+2}(\mathbf{x}) = \mathbf{x}_1^2, \\ &f_{n+3}(\mathbf{x}) = \mathbf{x}_1\mathbf{x}_2, \ldots, f_{2n+1}(\mathbf{x}) = \mathbf{x}_1\mathbf{x}_n, \\ &f_{2n+2}(\mathbf{x}) = \mathbf{x}_2^2, \\ &f_{2n+3}(\mathbf{x}) = \mathbf{x}_2\mathbf{x}_3, \ldots, f_{3n}(\mathbf{x}) = \mathbf{x}_2\mathbf{x}_n, \\ &\ldots, \ldots, f_p(\mathbf{x}) = \mathbf{x}_n^2. \end{aligned} \tag{12}$$

For the m samples $\mathbf{Y} = [\mathbf{Y}_1, \mathbf{Y}_2, \ldots, \mathbf{Y}_m]^T$ and $\mathbf{x} = [\mathbf{x}_1, \mathbf{x}_2, \ldots, \mathbf{x}_m]^T$, the regression basis function matrices are as follows:

$$\mathbf{f} = \begin{bmatrix} f_{1,1} & f_{1,2} & \cdots & f_{1,p} \\ f_{2,1} & f_{2,2} & \cdots & f_{2,p} \\ \vdots & \vdots & \ddots & \vdots \\ f_{m,1} & f_{m,2} & \cdots & f_{m,p} \end{bmatrix}_{m \times p}. \tag{13}$$

Further, the coefficient vectors $\boldsymbol{\beta}$ of the regression basis functions can be required from equation (14).

$$\boldsymbol{\beta} = \left(\mathbf{f}^T\mathbf{R}^{-1}\mathbf{f}\right)^{-1}\mathbf{f}^T\mathbf{R}^{-1}\mathbf{Y}. \tag{14}$$

3.1.4. Error Assessment. In summary, at arbitrary site $\mathbf{x}$, the local deviation of the prediction results given by the IK-RSM is

$$z(\mathbf{x}) = \mathbf{r}^T(\mathbf{x})\mathbf{R}^{-1}(\mathbf{Y} - \mathbf{f}\boldsymbol{\beta}), \tag{15}$$

where $\mathbf{r}(\mathbf{x}) = [R(\boldsymbol{\theta}, \mathbf{x}, \mathbf{x}_1), R(\boldsymbol{\theta}, \mathbf{x}, \mathbf{x}_2), \ldots, R(\boldsymbol{\theta}, \mathbf{x}, \mathbf{x}_m)]^T$ represents the correlation degree between arbitrary site $\mathbf{x}$ and the known sample point. According to the least squares estimation principle, the variance estimate value σ^2 of the Kriging model can be expressed as

$$\sigma^2 = \frac{1}{m}(\mathbf{Y} - \mathbf{f}\boldsymbol{\beta})^T\mathbf{R}^{-1}(\mathbf{Y} - \mathbf{f}\boldsymbol{\beta}). \tag{16}$$

3.2. Correction Coefficient Optimization of the Kernel Function Based on Genetic Algorithm. To accurately calculate the correction coefficient $\boldsymbol{\theta}_i$, the genetic algorithm is applied to find the optimum values of correction coefficients. For the m samples from n-dimensional variable, the Kriging model based on genetic algorithm is formulated as follows:

$$\begin{cases} \text{find} & \boldsymbol{\theta}_k \quad (k = 1, \ldots, n), \\ \min & \varphi(\boldsymbol{\theta}) = |R|^{1/m}\sigma^2, \\ \text{s.t.} & \boldsymbol{\theta}_k > 0. \end{cases} \tag{17}$$

The minimum fitness function is taken as the optimization objective, and the difficulty is to ensure that the error between the predicted value and the measured value is as small as possible in the process of parameter optimization, so as to ensure that the prediction accuracy of the established model meets the engineering requirements. It is possible for the objective function $\varphi(\theta)$ of the correction coefficient θ to be local optimum [21, 22]. Considering that the genetic algorithm is good at global optimization, based on the sample of sinking velocity, the correction coefficient θ of kernel function of Kriging model is optimized by using the genetic algorithm. The specific process is as follows in Figure 1.

As known from Figure 1, the specific solution process of Kriging correction coefficient based on genetic algorithm is as follows: according to the obtained data, select the sample data of relevant variables and normalize the data; define the optimization variable $\boldsymbol{\theta}$ in the solution process, code the variables, and initialize the population; calculate the fitness value according to the fitness

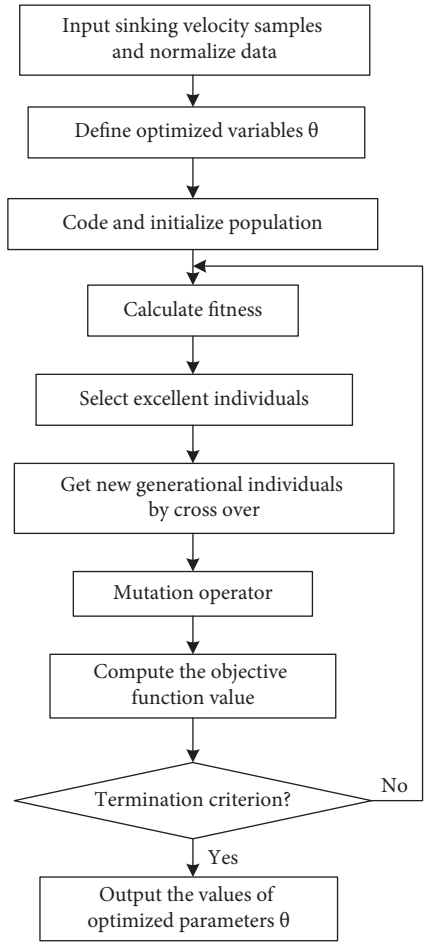

Figure 1: Optimization process of correction coefficient based on the genetic algorithm.

function; select the excellent individual in the population; generate the next generation of individuals to form the population through crossing operation; then carry out mutation operation, and calculate the objective function value; judge whether the objective function value meets the termination criterion; if not, perform the fitness value calculation again; if the criterion is met, the optimization parameter value is output.

3.3. Parameter Sensitivity Analysis. The gradient of the IK-RSM's interpolation results of the n-dimensional variable is

$$\frac{\partial \hat{y}(\mathbf{x})}{\partial \mathbf{x}} = \left[\frac{\partial \hat{y}(\mathbf{x})}{\partial \mathbf{x}_1}, \ldots, \frac{\partial \hat{y}(\mathbf{x})}{\partial \mathbf{x}_n}\right]^T. \tag{18}$$

Specifically, it can be expressed as

$$\frac{\partial \hat{y}(\mathbf{x})}{\partial \mathbf{x}} = \mathbf{J}_f(\mathbf{x})\boldsymbol{\beta} + \mathbf{J}_r(\mathbf{x})^T\boldsymbol{\gamma}, \tag{19}$$

where $\gamma = \mathbf{R}^{-1}(\mathbf{Y} - \mathbf{f}\boldsymbol{\beta})$; $\mathbf{J}_f(\mathbf{x})$ and $\mathbf{J}_r(\mathbf{x})$ are the partial derivative matrices of regression basis function vector $\mathbf{f}$ and kernel function vector $\mathbf{r}$ to the variable $\mathbf{x}$, respectively. Then, $\mathbf{J}_f(\mathbf{x})$ can be expressed as

$$J_f(\mathbf{x}) = \begin{bmatrix} \frac{\partial \mathbf{f}_1}{\partial \mathbf{x}_1} & \frac{\partial \mathbf{f}_2}{\partial \mathbf{x}_1} & \cdots & \frac{\partial \mathbf{f}_p}{\partial \mathbf{x}_1} \\ \frac{\partial \mathbf{f}_1}{\partial \mathbf{x}_2} & \frac{\partial \mathbf{f}_2}{\partial \mathbf{x}_2} & \cdots & \frac{\partial \mathbf{f}_p}{\partial \mathbf{x}_2} \\ \vdots & \vdots & \ddots & \vdots \\ \frac{\partial \mathbf{f}_1}{\partial \mathbf{x}_n} & \frac{\partial \mathbf{f}_2}{\partial \mathbf{x}_n} & \cdots & \frac{\partial \mathbf{f}_p}{\partial \mathbf{x}_n} \end{bmatrix}_{n\times p}. \tag{20}$$

Meanwhile, $\mathbf{J}_r(\mathbf{x})$ can be expressed as

$$\mathbf{J}_r(\mathbf{x}) = \left[\frac{\partial \mathbf{r}}{\partial \mathbf{x}_1} \ \frac{\partial \mathbf{r}}{\partial \mathbf{x}_2} \ \cdots \ \frac{\partial \mathbf{r}}{\partial \mathbf{x}_n}\right]_{m\times n}, \tag{21}$$

where $\mathbf{r}(\mathbf{x}) = [R(\boldsymbol{\theta}, \mathbf{x}, \mathbf{x}_1), R(\boldsymbol{\theta}, \mathbf{x}, \mathbf{x}_2), \ldots, R(\boldsymbol{\theta}, \mathbf{x}, \mathbf{x}_m)]^{\mathrm{T}}$.

Therefore, the estimated value of the total differential for response $y(\mathbf{x})$ is approximated as

$$\mathrm{d}\hat{y}(\mathbf{x}) = \sum_{i=1}^{n} \frac{\partial \hat{y}(\mathbf{x})}{\partial \mathbf{x}_i} \mathrm{d}\mathbf{x}_i. \tag{22}$$

$(\partial \hat{y}(\mathbf{x})/\partial \mathbf{x}_i)\mathrm{d}\mathbf{x}_i$ is the sensitivity of the response with the increasement $\mathrm{d}\mathbf{x}_i$ for the ith variable. Approximately, $\Delta\hat{y}(\mathbf{x}) = \sum_{i=1}^{n}(\partial \hat{y}(\mathbf{x})/\partial x_i)\Delta\mathbf{x}_i$ indicates the increment of the response with the increasement $\Delta\mathbf{x}_i$ of the ith variable.

4. Correlated Parameters Determination of the Sinking Velocity of F/A-18A

4.1. Deck Landing Parameters of F/A-18A. According to the MIL-A-8863C(AS) (Airplane Strength and Rigidity Ground Loads for Navy Acquired Airplanes), the definitions of sinking velocity and the engaging/approach velocity and carrier velocity are as follows.

The sinking velocity is the vertical velocity when the landing gear wheel of the aircraft touches the deck during landing; the unit is m/s.

The approach velocity is the horizontal velocity relative to the carrier when the aircraft and the arresting device are engaged during the landing process; the unit is m/s.

The engaging velocity is the composition of approach velocity and deck wind velocity component parallel to the deck center line direction; the unit is m/s.

The carrier velocity is the component of the actual carrier velocity in the deck center line direction; the unit is m/s too.

Based on the description of JSSG-2006, the following three types of 16 deck landing parameters are selected in the impact analysis of F/A-18A carrier-based aircraft [4].

4.1.1. Aircraft Attitude Parameters. Aircraft attitude parameters include approach velocity, engaging velocity, sinking velocity, landing weight, aircraft glide angle, aircraft pitch angle, aircraft roll angle, aircraft yaw angle, aircraft roll rate, aircraft pitch rate, and aircraft flight path angle.

4.1.2. Deck Landing Operation Parameters. Deck landing operation parameters include off-center engaging distance and ramp to touchdown distance.

4.1.3. Deck Landing Environmental Parameters. Deck landing environmental parameters include the deck pitch angle, the deck roll angle, and the carrier movement velocity.

4.2. Correlated Parameter Determination of the Sinking Velocity. In [4], 252 valid deck landing parameters samples of F/A-18A carrier-based aircraft are provided. Combined with the above partial correlation analysis, the results of the partial correlation coefficient calculation of the ship state parameters of the F/A-18A carrier aircraft (excluding the sinking velocity, a total of 15) and the sinking velocity of the ship are listed in Table 1.

From the partial correlation analysis results, it is found that the aircraft glide angle and deck pitch angle are highly correlated with the sinking velocity; next, the approach velocity and the engaging velocity are moderately correlated with the sinking velocity. The aircraft pitch rate, carrier velocity, landing weight, deck roll angle, aircraft roll angle, aircraft roll rate, aircraft pitch rate, aircraft pitch angle, aircraft yaw angle, ramp to touchdown distance, and off-center engaging distance are not correlated with the sinking velocity. Therefore, the key correlated parameters of the sinking velocity V_S of the F/A-18A carrier-based aircraft could be determined, including the aircraft glide angle C_G, the deck pitch angle C_P, the approach velocity V_A, and the engaging velocity V_E. The IK-RSM of these four parameters with the sinking velocity is further established, and the sensitivity of each correlated parameter will be calculated.

Table 1: Partial correlation analysis results between deck landing parameters and sinking velocity of F/A-18A.

No.	Parameters	Correlation coefficient	Correlation degree
1	Aircraft glide angle	0.988	Highly positive correlation
2	Deck pitch angle	−0.890	Highly negative correlation
3	Engaging velocity	0.561	Moderately positive correlation
4	Approach velocity	0.545	Moderately positive correlation
5	Aircraft pitch rate	−0.225	No
6	Carrier velocity	0.215	No
7	Landing weight	0.196	No
8	Deck roll angle	−0.094	No
9	Aircraft roll angle	−0.093	No
10	Aircraft roll rate	−0.084	No
11	Aircraft pitch rate	−0.064	No
12	Aircraft pitch angle	0.058	No
13	Aircraft yaw angle	−0.041	No
14	Ramp to touchdown distance	−0.041	No
15	Off-center engaging distance	−0.001	No

5. IK-RSM of the F/A-18A's Sinking Velocity and Sensitivity Analysis of the Correlated Parameters

5.1. The Deck Landing Parameters Statistical Characteristics of the F/A-18A. The 252 deck landing state samples of the F/A-18A carrier-based aircraft are shown in Tables 2 and 3, including 5 variables: the sinking velocity V_S, the aircraft glide angle C_G, the deck pitch angle C_P, the approach velocity V_A, and the engaging velocity V_E. The 126 samples from Table 2 are used to construct the IK-RSM of the sinking velocity, and the other 126 samples in Table 3 are used to verify the validation of the above model. The mean and standard deviation of each deck landing parameters are shown in Table 4.

5.2. IK-RSM of the Sinking Velocity. Considering the nonlinear relationship between the sinking velocity V_S and the other parameters including aircraft glide angle C_G, deck pitch angle C_P, approach velocity V_A, and engaging velocity V_E, the quadratic regression basis function is determined for the IK-RSM of the sinking velocity. According to the sample in Table 2, in the sinking velocity IK-RSM established, the sample number is $m = 126$, the variable number is $n = 4$, and the number of the regression basis functions is $p = 1/2(n+1)(n+2) = 15$. According to the sample, combined with equations (8), (9), and (11)–(13), the optimization model of correction coefficient θ for the kernel function of IK-RSM is as follows:

$$\begin{cases} \text{find} & \boldsymbol{\theta}_k \quad (k = 1, \ldots, 4), \\ \min & \varphi(\boldsymbol{\theta}) = |R|^{1/126}\sigma^2, \\ \text{s.t.} & \boldsymbol{\theta}_k > 0. \end{cases} \tag{23}$$

The optimization process of objective function is as follows.

By using the Lagrange multiplier method, the objective function converges to 0.065692 finally, and the convergence process is shown in Figure 2.

Furthermore, the genetic algorithm is employed, and the evolution process of the objective function is shown in Figure 3. The convergence of the objective function is achieved through 100 generations iterated, the convergence result is 0.060538, and the correction coefficient matrix $\theta = [\,363.683 \;\; 0.008 \;\; 493.786 \;\; 327.062\,]^T$. Therefore, $\mathbf{R}$ and $\boldsymbol{\beta}$ are as follows:

$$\mathrm{R} = \begin{bmatrix} 1 & 6.51 \times 10^{-24} & \cdots & 1.64 \times 10^{-79} \\ 6.51 \times 10^{-24} & 1 & \cdots & 3.41 \times 10^{-75} \\ \vdots & \vdots & \ddots & \vdots \\ 1.64 \times 10^{-79} & 3.41 \times 10^{-75} & \cdots & 1 \end{bmatrix}_{126\times126},$$

$$\boldsymbol{\beta} = [\,-0.024 \;\; -0.023 \;\; 0.221 \;\; 1.012 \;\; -0.246 \;\; -0.017 \;\; -0.038 \;\; -0.062 \;\; 0.111 \;\; 0.064 \;\; 0.113 \;\; -0.141 \;\; 0.004 \;\; -0.029 \;\; 0.036\,]^T_{15\times1}, \tag{24}$$

Table 2: The sinking velocity and correlated parameters sample for IK-RSM construction.

No.	V_S (m/s)	V_A (m/s)	V_E (m/s)	C_G (Rad)	C_P (Rad)
1	1.6	77	63	0.022	−0.002
2	1.6	82	68	0.008	−0.014
3	2	75	59	0.024	−0.007
4	2.1	77	61	0.027	−0.007
5	2.2	74	63	0.03	−0.003
6	2.4	69	59	0.036	−0.002
7	2.4	77	61	0.027	−0.009
8	2.4	77	62	0.03	−0.009
9	2.5	81	65	0.03	−0.002
10	2.6	76	60	0.03	−0.01
11	2.6	79	65	0.033	−0.005
12	2.7	75	59	0.039	−0.005
13	2.7	75	61	0.039	−0.005
14	2.7	76	62	0.038	−0.005
15	2.7	78	62	0.033	−0.005
16	2.7	79	63	0.034	0
17	2.7	81	66	0.038	−0.002
18	2.8	71	58	0.039	−0.009
19	2.8	75	60	0.04	−0.007
20	2.8	75	62	0.043	−0.002
21	2.8	78	64	0.038	−0.005
22	2.9	72	57	0.038	−0.007
23	2.9	73	61	0.05	0.002
24	2.9	77	63	0.036	−0.009
25	2.9	77	65	0.039	−0.003
26	3	70	59	0.044	−0.005
27	3.1	74	59	0.043	−0.009
28	3.1	75	59	0.038	−0.005
29	3.1	72	61	0.047	−0.002
30	3.1	74	61	0.046	−0.003
31	3.1	75	63	0.051	0.002
32	3.1	79	64	0.045	−0.003
33	3.2	70	55	0.049	−0.009
34	3.2	76	60	0.041	−0.009
35	3.2	76	60	0.048	−0.005
36	3.2	74	63	0.043	−0.003
37	3.2	76	64	0.042	−0.007
38	3.2	79	64	0.04	−0.01
39	3.2	78	66	0.041	−0.005
40	3.2	81	67	0.041	0
41	3.2	82	69	0.033	−0.009
42	3.3	70	59	0.054	−0.002
43	3.3	74	59	0.048	−0.007
44	3.3	73	60	0.046	−0.007
45	3.3	76	61	0.05	−0.005
46	3.3	77	61	0.049	−0.005
47	3.3	78	62	0.046	−0.003
48	3.3	78	63	0.044	−0.009
49	3.4	68	57	0.055	−0.005
50	3.4	72	58	0.055	−0.003
51	3.4	74	59	0.05	−0.003
52	3.4	75	59	0.054	−0.003
53	3.4	78	64	0.044	−0.009
54	3.4	82	69	0.042	−0.005
55	3.5	70	56	0.056	−0.007
56	3.5	73	59	0.052	−0.007
57	3.5	73	59	0.044	−0.009
58	3.5	73	60	0.057	−0.002
59	3.5	75	63	0.046	−0.009
60	3.5	76	64	0.052	−0.002
61	3.5	79	65	0.041	−0.005
62	3.5	78	66	0.05	−0.003
63	3.6	76	60	0.058	−0.002
64	3.6	73	62	0.052	−0.005
65	3.6	76	62	0.037	−0.009
66	3.6	76	62	0.055	−0.003
67	3.6	74	64	0.055	−0.003
68	3.6	77	64	0.05	−0.003
69	3.6	77	64	0.048	−0.005
70	3.7	71	56	0.06	−0.005
71	3.7	72	59	0.048	−0.012
72	3.7	76	60	0.054	−0.003
73	3.7	76	61	0.049	−0.01
74	3.7	76	62	0.054	−0.007
75	3.7	76	63	0.05	−0.009
76	3.7	82	69	0.04	−0.01
77	3.8	75	59	0.054	−0.009
78	3.8	72	60	0.054	−0.009
79	3.8	73	60	0.048	−0.007
80	3.8	76	61	0.055	−0.005
81	3.8	79	64	0.048	−0.01
82	3.9	71	60	0.062	−0.003
83	3.9	75	60	0.053	−0.009
84	3.9	76	60	0.056	−0.009
85	4	71	59	0.061	−0.007
86	4	76	61	0.057	−0.01
87	4	74	62	0.046	−0.002
88	4	76	62	0.061	−0.003
89	4	75	63	0.063	0
90	4	76	64	0.058	−0.003
91	4	79	65	0.058	−0.007
92	4	82	66	0.056	−0.003
93	4.1	71	59	0.067	−0.002
94	4.1	72	60	0.063	−0.005
95	4.1	73	61	0.061	−0.005
96	4.1	76	62	0.054	−0.009
97	4.1	77	64	0.056	−0.007
98	4.1	79	64	0.05	−0.012
99	4.2	74	61	0.062	−0.005
100	4.2	74	62	0.062	−0.003
101	4.2	75	63	0.066	−0.002
102	4.2	78	65	0.045	−0.012
103	4.3	71	58	0.062	−0.009
104	4.3	74	62	0.057	−0.012
105	4.3	78	63	0.05	−0.012
106	4.3	78	64	0.05	−0.01
107	4.3	78	65	0.061	−0.005
108	4.4	76	62	0.063	−0.007
109	4.4	77	62	0.061	−0.005
110	4.4	78	62	0.067	−0.002
111	4.5	70	59	0.07	−0.007
112	4.6	69	58	0.074	−0.003
113	4.6	79	65	0.066	−0.007
114	4.7	73	59	0.063	−0.01
115	4.7	74	61	0.064	−0.003
116	4.7	75	63	0.07	−0.003
117	4.7	75	63	0.073	0.003
118	4.8	70	58	0.062	−0.005
119	4.8	74	62	0.068	−0.003

Table 2: Continued.

No.	V_S (m/s)	V_A (m/s)	V_E (m/s)	C_G (Rad)	C_P (Rad)
120	4.8	77	65	0.061	−0.007
121	4.9	71	55	0.08	−0.002
122	4.9	80	65	0.066	−0.007
123	5	78	66	0.069	−0.003
124	5.1	70	56	0.08	−0.009
125	5.5	76	62	0.079	−0.009
126	5.5	79	63	0.078	−0.009

Table 3: The sinking velocity and correlated parameters sample for IK-RSM validation.

No.	V_S (m/s)	V_A (m/s)	V_E (m/s)	C_G (Rad)	C_P (Rad)
127	2	77	63	0.026	−0.003
128	2.4	76	62	0.034	−0.003
129	2.6	73	60	0.037	−0.003
130	2.8	78	62	0.04	−0.002
131	2.8	76	60	0.039	−0.003
132	2.8	78	64	0.032	−0.01
133	2.9	74	59	0.037	−0.01
134	2.9	80	66	0.036	−0.003
135	3	77	62	0.04	−0.007
136	3	77	62	0.034	−0.014
137	3	83	68	0.038	−0.003
138	3.1	71	56	0.05	−0.003
139	3.1	76	63	0.039	−0.005
140	3.1	75	63	0.039	−0.007
141	3.1	78	63	0.042	−0.005
142	3.2	74	61	0.049	−0.002
143	3.2	76	62	0.044	−0.007
144	3.2	76	62	0.044	−0.005
145	3.2	73	61	0.048	−0.003
146	3.2	74	60	0.05	−0.002
147	3.2	76	61	0.046	−0.007
148	3.2	79	65	0.038	−0.009
149	3.2	73	58	0.05	−0.003
150	3.3	79	67	0.042	−0.003
151	3.3	74	60	0.045	−0.009
152	3.3	76	64	0.041	−0.005
153	3.3	71	60	0.048	−0.005
154	3.3	78	62	0.038	−0.014
155	3.3	75	61	0.042	−0.007
156	3.3	80	64	0.038	−0.012
157	3.4	70	59	0.046	−0.01
158	3.4	74	61	0.047	−0.007
159	3.4	76	63	0.046	−0.005
160	3.4	78	65	0.049	−0.002
161	3.4	72	58	0.05	−0.005
162	3.4	75	59	0.043	−0.01
163	3.4	75	62	0.044	−0.009
164	3.4	82	69	0.043	−0.005
165	3.4	78	63	0.044	−0.007
166	3.5	74	60	0.051	−0.005
167	3.5	77	62	0.047	−0.007
168	3.5	72	57	0.054	−0.005
169	3.5	75	63	0.042	−0.01
170	3.5	75	63	0.048	−0.005
171	3.5	77	64	0.044	−0.009
172	3.5	75	63	0.049	−0.005
173	3.5	74	62	0.045	−0.01
174	3.5	76	65	0.048	−0.005
175	3.6	74	59	0.056	−0.003
176	3.6	75	60	0.051	−0.009
177	3.6	75	63	0.053	−0.003
178	3.6	73	59	0.048	−0.012
179	3.6	75	61	0.052	−0.005
180	3.6	76	63	0.049	−0.007
181	3.6	82	68	0.036	−0.014
182	3.7	75	62	0.047	−0.01
183	3.7	76	64	0.049	−0.007
184	3.7	77	65	0.051	−0.003
185	3.7	69	57	0.062	0
186	3.7	74	58	0.053	−0.007
187	3.7	75	61	0.048	−0.009
188	3.7	76	63	0.054	−0.003
189	3.7	80	65	0.046	−0.009
190	3.7	79	63	0.049	−0.007
191	3.8	75	61	0.055	−0.005
192	3.8	72	58	0.057	−0.003
193	3.8	73	60	0.051	−0.007
194	3.8	74	63	0.053	−0.003
195	3.8	76	63	0.05	−0.007
196	3.8	76	64	0.052	−0.003
197	3.8	82	67	0.05	−0.005
198	3.8	73	59	0.057	−0.005
199	3.9	74	61	0.052	−0.01
200	3.9	70	56	0.059	−0.005
201	3.9	73	58	0.061	−0.003
202	4	68	57	0.064	−0.003
203	4	72	56	0.06	−0.009
204	4	75	62	0.057	−0.003
205	4	75	60	0.057	−0.007
206	4	74	62	0.057	−0.007
207	4	75	61	0.058	−0.005
208	4	74	59	0.057	−0.007
209	4.1	74	60	0.058	−0.009
210	4.1	75	62	0.051	−0.012
211	4.1	74	60	0.062	−0.003
212	4.1	74	62	0.056	−0.005
213	4.1	77	63	0.056	−0.007
214	4.2	72	60	0.061	−0.007
215	4.2	74	61	0.057	−0.01
216	4.2	78	62	0.063	−0.003
217	4.2	71	57	0.062	−0.01
218	4.2	73	58	0.065	−0.007
219	4.2	75	64	0.055	−0.009
220	4.2	78	63	0.061	−0.005
221	4.2	70	59	0.065	−0.005
222	4.2	74	60	0.06	−0.007
223	4.3	72	60	0.061	−0.009
224	4.3	74	58	0.068	−0.003
225	4.3	75	60	0.057	−0.012
226	4.3	73	61	0.065	−0.002
227	4.3	74	62	0.058	−0.009
228	4.3	75	63	0.062	−0.005
229	4.4	71	60	0.063	−0.009
230	4.4	74	62	0.062	−0.005
231	4.4	73	60	0.063	−0.007
232	4.4	78	65	0.059	−0.003
233	4.4	75	62	0.066	−0.005

Table 3: Continued.

No.	V_S (m/s)	V_A (m/s)	V_E (m/s)	C_G (Rad)	C_P (Rad)
234	4.4	72	61	0.065	−0.005
235	4.5	76	64	0.066	−0.003
236	4.5	73	61	0.06	−0.01
237	4.6	73	62	0.069	−0.005
238	4.6	77	65	0.064	−0.003
239	4.7	76	62	0.068	−0.005
240	4.7	79	63	0.068	−0.005
241	4.7	76	63	0.068	−0.003
242	4.8	75	63	0.064	−0.01
243	4.8	75	61	0.068	−0.009
244	4.9	73	59	0.075	−0.007
245	4.9	75	60	0.074	−0.005
246	4.9	73	61	0.076	−0.003
247	5	74	62	0.073	−0.005
248	5	77	65	0.067	−0.007
249	5.2	72	62	0.07	−0.009
250	5.3	75	62	0.077	−0.007
251	5.4	73	60	0.085	−0.003
252	5.6	78	65	0.084	0

Table 4: The mean and standard deviation of the F/A-18A deck landing parameters.

	Sinking velocity V_S (m/s)	Approach velocity V_A (m/s)	Engaging velocity V_E (m/s)	Aircraft glide angle C_G (Rad)	Deck pitch angle C_P (Rad)
Mean	3.70	75.22	61.67	0.052	−0.006
Standard deviation	0.71	2.88	2.68	0.012	0.003

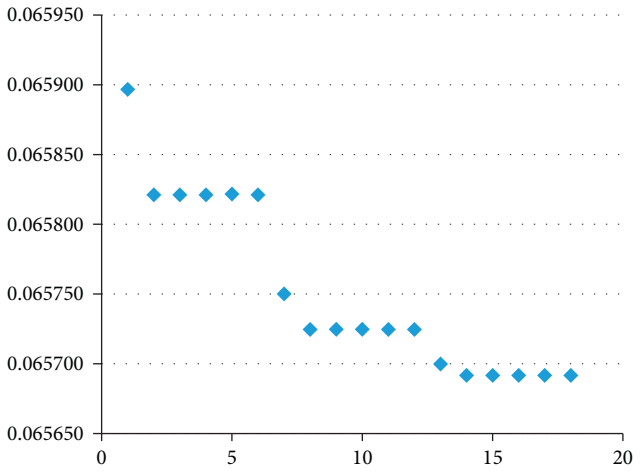

Figure 2: The convergence process of objective function by using Lagrange multiplier method.

where the matrix **R** is practically the "identity matrix": 1 in the main diagonal and about 0 as other coefficients.

5.3. Error Assessment and Comparison with Other Models. 126 samples in Table 3 are used to verify the IK-RSM of sinking velocity. Meanwhile, the sinking velocity empirical formula provided by [20] and the ordinary Kriging model are compared with the IK-RSM. The measured data of aircraft glide angle C_G, deck pitch angle C_P, approach velocity V_A, and engaging velocity V_E in Table 3 are replaced in the above models, respectively. The measured data of sinking velocity and the prediction results of various models are shown in Figure 4. The error comparisons are shown in Figure 5 and Table 5.

The compared results in Table 5 show that, compared with the empirical formula provided by [20] and the Kriging model, the sinking velocity prediction accuracy indexes of IK-RSM are the best, including the coefficient of determination (the coefficient of determination is more close to 1, which means higher precision), the mean relative error, and the maximum relative error. Therefore, by using the IK-RSM, we can get the sinking velocity prediction model with the various parameters including aircraft glide angle C_G, deck pitch angle C_P, approach velocity V_A, and engaging velocity V_E.

It is too complex to deduce the sinking velocity according to the related theory of the aircraft conceptual design and flight mechanics, which is unable to accomplish analysis effectively. Based on the measured data, through the partial correlation analysis and the IK-RSM model of the sinking velocity in this paper, the internal relationship between the sinking velocity and the other deck landing parameters can be primarily obtained; that is, the sinking velocity is the vertical component of the engaging velocity, and it is also related to the glide angle and the deck pitch angle of the aircraft during the deck landing process and also including the random error compensation of Kriging model. Compared with the empirical formula, the predicted results from the IK-RSM model are more consistent with the measured value. The sensitivity analysis of the above parameters can be further carried out.

5.4. Sensitivity Analysis Results. According to equation (18), the gradient of sinking velocity can be obtained at all correlated parameters. If the correlated parameters have a certain increment, the corresponding increment of sinking velocity can be obtained according to the above gradient, that is, the sensitivity of each variable. Furthermore, according to equation (22), we can get the increment of sinking velocity when all correlated variables vary at the same time. Hence, Table 6 shows the influence degree of sinking velocity due to 1% increment at the mean of each correlated parameter.

The samples in Tables 1 and 2 have been sorted from small to large according to the sinking velocity, and all 252 samples are determined. According to the sensitivity analysis of the parameters related to the sinking velocity of all 252 samples, the increment of the sinking velocity can be calculated at 1% of the variation of each variable from each sample. The calculation results are shown in Figure 6. The average influence degree of the correlated parameters can be calculated from the 252 samples, as shown in Figure 7. It can be seen that the sensitivity of the engaging velocity V_E is the greatest, that of the aircraft glide angle C_G is the second, that

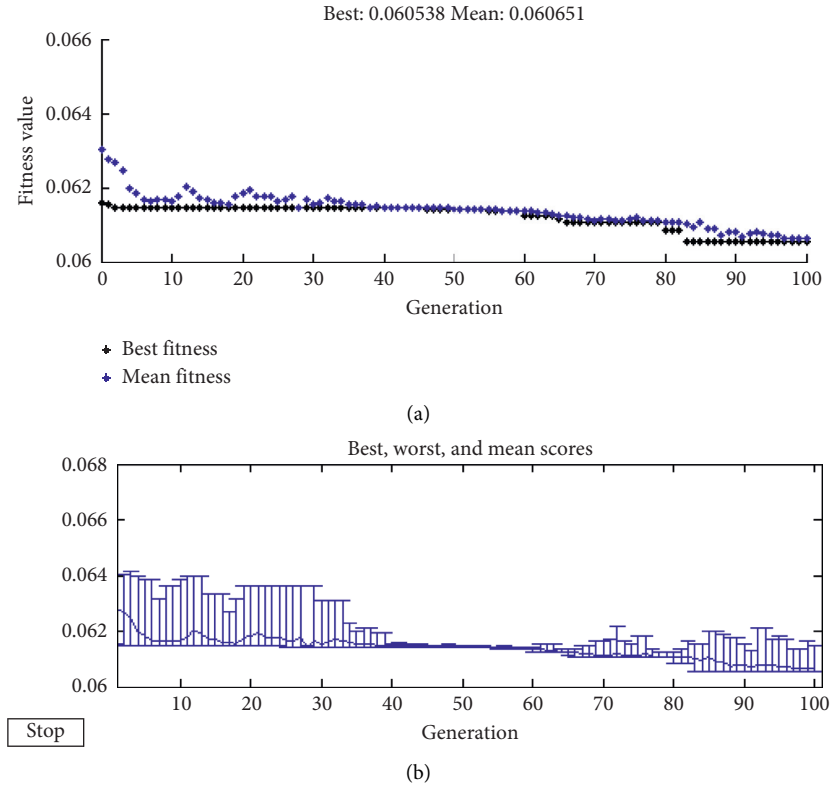

Figure 3: The convergence process of objective function by using genetic algorithm.

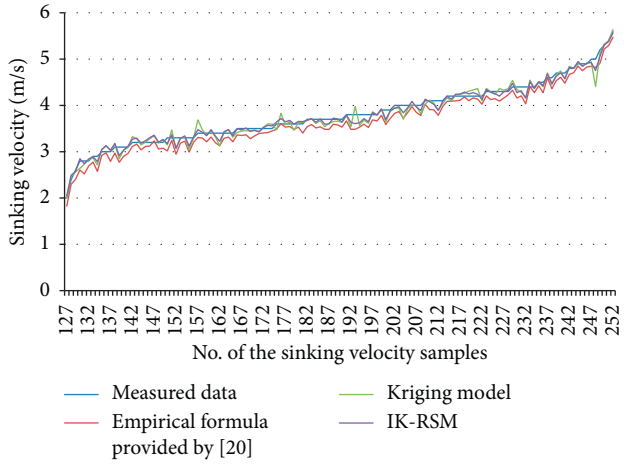

Figure 4: Comparison of the sinking velocity measured data with the prediction results of various models.

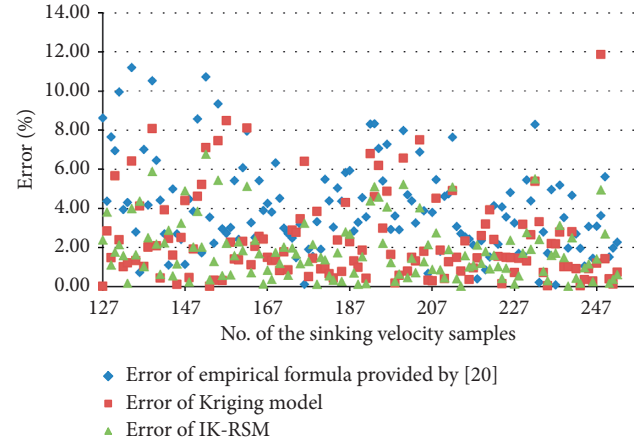

Figure 5: Error comparison of the various models for the sinking velocity.

of the deck pitch angle C_P is the third, and that of the approach velocity V_A is the least. The above analysis means that the sinking velocity is most sensitive to the engaging velocity V_E.

From the sensitivity curve of Figure 6, it can be seen that there is a big sudden change in the influence degree on the sinking velocity at the No. 225 and No. 242 samples, and the increment of the sinking velocity reaches 0.2527 m/s and 0.31 m/s, respectively. The above two sample points and their adjacent samples are listed in Table 7. The parameters of the two samples and their adjacent samples also have a big sudden change, including the approach velocity, the engaging velocity, the aircraft glide angle, and the deck pitch angle. Therefore, the influence degree of each parameter on sinking velocity has a sudden change, which leads to a big change in sensitivity analysis results at the two sample points.

As shown in Figure 6, there is a contradictory phenomenon that when the approach velocity increases, the sinking velocity decreases at some samples. As shown in Table 8, in the case that the engaging velocity, aircraft glide angle, and deck pitch angle are constant, for the samples No.

Table 5: Comparison of sinking velocity prediction results.

Sinking velocity resource	Measured data	Empirical formula provided by [20]	Kriging model	IK-RSM
Mean (m/s)	3.814	3.667	3.786	3.805
Mean square deviation (m/s)	0.641	0.651	0.644	0.635
Coefficient of determination $\mathbf{R}^2$	—	0.934	0.964	0.981
Mean relative error $(1/126)\sum_{i=1}^{126}\lvert(V_{S,i}^{*} - V_{S,i})/V_{S,i} \times 100\%\rvert$	—	4.004%	2.343%	1.813%
Maximum relative error $\max_{i=1}^{126}(\lvert(V_{S,i}^{*} - V_{S,i})/V_{S,i}\rvert \times 100\%)$	—	11.196%	11.865%	6.771%

Table 6: The influence degree of the correlated parameters on the sinking velocity.

No.	Correlated parameter	Mean	Gradient at the mean of each correlated parameter	Sinking velocity increment due to 1% increment at the mean of each correlated parameter (m/s)
1	Approach velocity V_A	75.22 (m/s)	5.3177×10^{-4}	4.0102×10^{-4}
2	Engaging velocity V_E	61.67 (m/s)	0.0541	3.3419×10^{-2}
3	Aircraft glide angle C_G	0.052 (Rad)	60.0809	3.0269×10^{-2}
4	Deck pitch angle C_P	−0.006 (Rad)	−56.0828	3.1780×10^{-3}
Sum	—	—	—	6.7267×10^{-2}

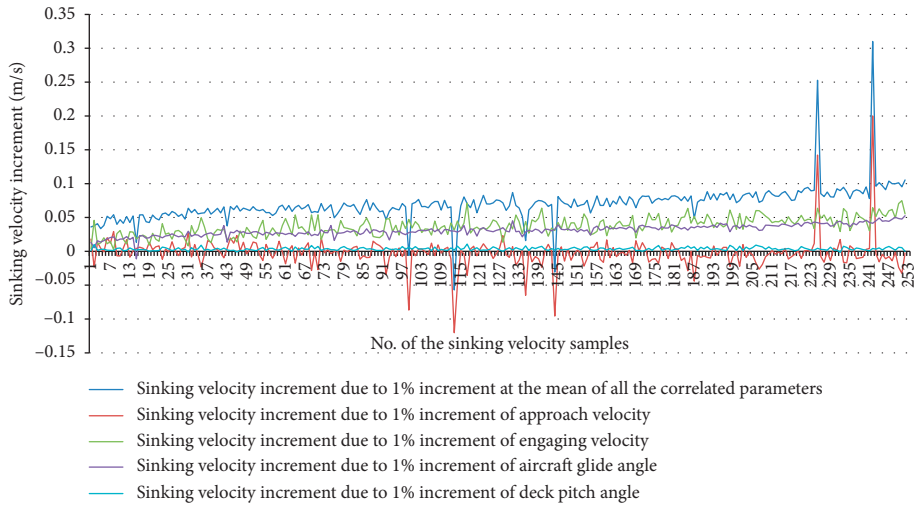

Figure 6: The sinking velocity increment at 1% of the variation of each variable from 252 samples.

144 and No. 113, the approach velocity increases from 74 m/s to 75 m/s, and, according to the general proportional relationship between the approach velocity and the sinking velocity, the sinking velocity should increase. However, the measured value of sinking velocity decreases from 3.8 m/s to 3.6 m/s. Here, it can be seen that, in the sensitivity analysis results of various variables correlated with sinking velocity, the increment of sinking velocity is −0.0957 m/s when the engaging velocity V_A increases 1%, which indicates that the sinking velocity has a decreasing trend under these circumstances. Similarly, for samples No. 187 and No. 168, the approach velocity increased from 74 m/s to 76 m/s; however, the measured value of sinking velocity decreases from 4.2 m/s to 4 m/s. It also can be seen that, in the sensitivity analysis results of various variables correlated with sinking velocity, the increment of sinking velocity is −0.0441 m/s when the engaging velocity V_A increases 1%. Therefore, through the sinking velocity IK-RSM and the sensitivity analysis method proposed, we have explained the contradictory phenomenon that when the approach velocity increases, the sinking velocity decreases at some samples. It could provide certain technical support for the flight attitude control related to the sinking velocity during the actual flight of carrier-based aircraft.

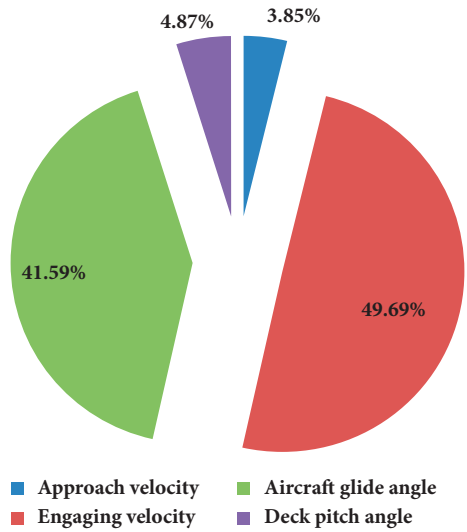

Figure 7: The average influence degree of each correlated parameter on sinking velocity.

Table 7: The samples whose influence degree on sinking velocity has a sudden change.

No.	Sinking velocity V_S (m/s)	Approach velocity V_A (m/s)	Engaging velocity V_E (m/s)	Aircraft glide angle C_G (Rad)	Deck pitch angle C_P (Rad)	Sinking velocity increment when each parameter varies 1% at the same time (m/s)
224	4.6	69	58	0.074	−0.003	0.0901
225	4.6	79	65	0.066	−0.007	0.2527
226	4.7	76	62	0.068	−0.005	0.0852
241	4.9	71	55	0.08	−0.002	0.0779
242	4.9	80	65	0.066	−0.007	0.3100
243	5	74	62	0.073	−0.005	0.0961

Table 8: The samples demonstrating the phenomenon that when the approach velocity increases, the sinking velocity decreases.

No.	Sinking velocity V_S (m/s)	Approach velocity V_A (m/s)	Engaging velocity V_E (m/s)	Aircraft glide angle C_G (Rad)	Deck pitch angle C_P (Rad)	Sinking velocity increment due to 1% increment of the approach velocity (m/s)
144	3.8	74	63	0.053	−0.003	−0.0957
113	3.6	75	63	0.053	−0.003	−0.1202
187	4.2	74	61	0.057	−0.01	−0.0441
168	4	76	61	0.057	−0.01	−0.0169

6. Conclusion

The deck landing sinking velocity of carrier-based aircraft is affected by aircraft carrier attitude, sea condition, and aircraft performance. Based on the deck landing measured data of the F/A-18A aircraft, the influence degree of the deck landing parameters on the sinking velocity under the actual operating environment has been explored, by using the partial correlation analysis of multivariate statistical theory and the IK-RSM of the sinking velocity, and the following conclusions are formed:

(1) It can be found that the 4 parameters are strongly correlated with the sinking velocity: the aircraft glide angle, the deck pitch angle, the engaging velocity, and the approach velocity, and the mentioned parameters could be used to establish the impact analysis model of the sinking velocity.

(2) The genetic algorithm is applied to the correction coefficients optimization of the kernel functions, and the IK-RSM of sinking velocity is formed and can be used to predict the sinking velocity of the carrier-based aircraft. Compared with the empirical formula and the Kriging model, the sinking velocity prediction accuracy indexes of IK-RSM are the best; for example, the coefficient of determination is 0.981 (the coefficient of determination is more close to 1, which means higher precision), the mean relative error is 1.813%, and the maximum relative error is 6.771%.

(3) Through the sensitivity analysis of the IK-RSM of the F/A-18A aircraft sinking velocity, it can be seen that the sensitivity of the engaging velocity V_E is the greatest, that of the aircraft glide angle C_G is the second, that of the deck pitch angle C_P is the third, and that of the approach velocity V_A is the least. Furthermore, through the sensitivity analysis method proposed and the gradient of sinking velocity at all correlated parameters, we have explained the contradictory phenomenon that when the approach velocity increases, the sinking velocity decreases at some samples. It could provide certain technical support for the flight attitude control related to the sinking velocity during the actual flight of carrier-based aircraft.

Data Availability

The data used to support the findings of this study are available from the corresponding author upon request.

Conflicts of Interest

The authors declare that they have no conflicts of interest.

References

[1] A. J. Gooday and A. Moguilevsky, "The sinking velocities of some halocyprid ostracods," *Journal of Experimental Marine Biology and Ecology*, vol. 19, no. 2, pp. 105–116, 1975.

[2] MIL-A-8863C (AS), *Airplane Strength and Rigidity, Ground Loads for Navy Acquired Airplanes*, Naval Air Systems Command, Patuxent River, MD, USA, 1993.

[3] JSSG-2006, *Aircraft Structures*, Naval Air Systems Command, Patuxent River, MD, USA, 1998.

[4] R. P. Micklos, *Carrier Landing Parameters From Survey 45, Fleet And Training Command Aircraft Landing Aboard USS Enterprise CVN-65 (Appendices B Through R)*, Naval Air Development Center Warminster PA Air Vehicle and Crew Systems Technology Dept, Fort Belvoir, VA, USA, 1991.

[5] J. Z. Geng, H. L. Yao, and Z. Y. Duan, "Determining the approach speed envelope of carrier aircraft," *Engineering Sciences*, vol. 11, no. 6, pp. 19–23, 2013.

[6] G. Xia, R. Dong, J. Xu, and Q. Zhu, "Linearized model of carrier-based aircraft dynamics in final-approach air condition," *Journal of Aircraft*, vol. 53, no. 1, pp. 33–47, 2016.

[7] Z. Q. Wang, X. Y. Sun, S. Zhou, and H. S. Lei, "Dynamics analysis of aircraft landing on the pitching deck," *Key Engineering Materials*, vol. 467–469, pp. 579–582, 2011.

[8] Q. D. Zhu, X. Meng, and Z. Zhang, "Simulation research on motion law of arresting hook during landing," *Applied Mechanics and Materials*, vol. 300-301, pp. 997–1002, 2013.

[9] L. Wang, Q. Zhu, Z. Zhang, and R. Dong, "Modeling pilot behaviors based on discrete-time series during carrier-based aircraft landing," *Journal of Aircraft*, vol. 53, no. 6, pp. 1922–1931, 2016.

[10] W. Zhang, Z. Zhang, Q. D. Zhu, and X. Shiyue, "Dynamics model of carrier-based aircraft landing gears landed on dynamic deck," *Chinese Journal of Aeronautics*, vol. 22, no. 4, pp. 371–379, 2009.

[11] Y. Wang, W. Wang, and X. Qu, "Multi-body dynamic system simulation of carrier-based aircraft ski-jump takeoff," *Chinese Journal of Aeronautics*, vol. 26, no. 1, pp. 104–111, 2013.

[12] L. Q. Yang, Z. Y. Zhen, K. W. Li, and C. Jia, "Carrier-based aircraft ski-jump take-off control system and visual simulation," in *Proceedings of the IEEE Chinese Guidance, Navigation and Control Conference*, Nanjing, China, August 2016.

[13] K. Yue, Y. Sun, H. Liu, and W. Guo, "Analysis of the flow field of carrier-based aircraft exhaust jets impact on the flight deck," *International Journal of Aeronautical and Space Sciences*, vol. 16, no. 1, pp. 1–7, 2015.

[14] H. T. Yin, X. M. Wang, W. C. Li et al., "Study of disturbances model on carrier-based aircraft landing process," in *Proceedings of the International Conference on Mechatronics and Industrial Informatics*, Guangzhou, China, March 2013.

[15] X. Wang, X. Chen, and L. Y. Wen, "Adaptive disturbance rejection control for automatic carrier landing system," *Mathematical Problems in Engineering*, vol. 2016, Article ID 7345056, 12 pages, 2016.

[16] T. W. Simpson, T. M. Mauery, J. Korte, and F. Mistree, "Kriging models for global approximation in simulation-based multidisciplinary design optimization," *AIAA Journal*, vol. 39, no. 12, pp. 2233–2241, 2001.

[17] C. Lu, Y.-W. Feng, R. P. Liem, and C.-W. Fei, "Improved Kriging with extremum response surface method for structural dynamic reliability and sensitivity analyses," *Aerospace Science and Technology*, vol. 76, pp. 164–175, 2018.

[18] T.-Y. Lee and H.-W. Shen, "Efficient local statistical analysis via integral histograms with discrete wavelet transform," *IEEE Transactions on Visualization and Computer Graphics*, vol. 19, no. 12, pp. 2693–2702, 2013.

[19] B. Keshtegar and S. Chakraborty, "A hybrid self-adaptive conjugate first order reliability method for robust structural reliability analysis," *Applied Mathematical Modelling*, vol. 53, pp. 319–332, 2018.

[20] Y. Feng, S. Liu, H. Xue, and S. Cui, "Sinking velocity impact anaysis of carrier-based aircraft based on test data," *Acta Aeronautica et Astronautica Sinica*, vol. 36, no. 11, pp. 3578–3585, 2015, in Chinese.

[21] D. Meng, S. Yang, Y. Zhang, and S. P. Zhu, "Structural reliability analysis and uncertainties-based collaborative design and optimization of turbine blades using surrogate model," *Fatigue & Fracture of Engineering Materials & Structures*, vol. 42, no. 6, pp. 1219–1227, 2019.

[22] R. Liu, P. Chen, X. Zhang, and S. Zhu, "Non-shock ignition probability of octahydro-1,3,5,7-tetranitro-tetrazocine-based polymer bonded explosives based on microcrack stochastic distribution," *Propellants, Explosives, Pyrotechnics*, vol. 45, no. 4, pp. 568–580. In press, 2020.